EUROPEAN ORGANIZATION FOR NUCLEAR RESEARCH

CERN-EP-2016-xxx
5 December 2016

Systematic studies of correlations between different order flow harmonics in Pb–Pb collisions at $\sqrt{s_{\rm NN}} = 2.76$ TeV

ALICE Collaboration*

Abstract

The correlations between event-by-event fluctuations of amplitudes of anisotropic flow harmonics have been measured in Pb–Pb collisions at $\sqrt{s_{\rm NN}} = 2.76$ TeV with the ALICE detector at the Large Hadron Collider. The results were obtained with the multi-particle correlation observables dubbed symmetric cumulants. These observables are robust against ~~systematic~~ biases originating from non-flow effects. The centrality dependence of correlations between the higher order harmonics (v_3, v_4 and v_5) and the lower order harmonics (v_2 and v_3) as well as the transverse momentum dependence of correlations of v_3 and v_2, v_4 and v_2 ~~correlations~~ are presented. The results are compared to calculations from viscous hydrodynamics and A Multi-Phase Transport (AMPT) model calculations. The comparison to viscous hydrodynamic model demonstrates that the different order harmonic correlations respond differently to the initial conditions of the temperature dependence of the shear viscosity to ~~the~~ entropy density ~~ratio~~ (η/s). The small η/s regardless of initial conditions is favored and the ~~small η/s with the~~ AMPT initial condition is closest to the measurements. Correlations between v_2, v_3 and v_4 ~~magnitudes~~ show moderate $p_{\rm T}$ dependence in mid-central collisions. This might be an indication of possible viscous corrections ~~for~~ the equilibrium distribution at hadronic freeze-out, which might help to understand possible contribution of bulk viscosity in a hadronic phase of the system. Together with the existing measurements of individual flow harmonics, the presented results provide further constraints on initial conditions and the transport properties of the system produced in heavy-ion collisions.

*when I write word1/word2 ; it means word1 and word2 should be swapped

* all the text in all the figures must be made larger!

*See Appendix A for the list of collaboration members

1 Introduction

The main emphasis of the ultra-relativistic heavy-ion collisions at the Relativistic Heavy Ion Collider (RHIC) and the Large Hadron Collider (LHC) is to study deconfined phase of the strongly interacting nuclear matter, the Quark-Gluon Plasma (QGP). This matter exhibits strong collective and anisotropic flow in the plane transverse to the beam direction, which is driven by the anisotropic pressure gradients, resulting in more particles emitted in the direction of the largest gradients. The large elliptic flow discovered at RHIC energies [1] continues to increase also at LHC energies [2, 3]. This has been predicted by calculations utilizing viscous hydrodynamics [4–9]. These calculations also demonstrated that the shear viscosity to the entropy density ratio (η/s) of QGP is close to a universal lower bound $1/4\pi$ [10] in heavy-ion collisions at RHIC and LHC energies.

The temperature dependence of the η/s has some generic features that most of the known fluids obey. For instance, one such general behavior is that the ratio typically reaches its minimum value close to the phase transition region [11]. It was shown, using kinetic theory and quantum mechanical considerations [12], that $\eta/s \sim 0.1$ would be the correct order of magnitude for the lowest possible shear viscosity to entropy ratio value found in nature. Later it was demonstrated that an exact lower bound $(\eta/s)_{\rm min} = 1/4\pi \approx 0.08$ can be calculated using the AdS/CFT correspondence [10]. Hydrodynamical simulations support as well the view that η/s of the QGP matter is close to that limit [8]. This may have important implications for other fundamental physics goals. It is argued that such a low value might imply that thermodynamic trajectories for the expanding matter would lie close to the quantum chromodynamics (QCD) critical end point, which is another subject of intensive experimental quest [11, 13].

Anisotropic flow [14] is traditionally quantified with $n^{\rm th}$-order flow coefficients v_n and corresponding symmetry plane angles Ψ_n in the Fourier decomposition of particle azimuthal distribution in the plane transverse to the beam direction [15]:

$$E\frac{{\rm d}^3N}{{\rm d}p^3} = \frac{1}{2\pi}\frac{{\rm d}^2N}{p_{\rm T}{\rm d}p_{\rm T}{\rm d}\eta}\left\{1+2\sum_{n=1}^{\infty} v_n(p_{\rm T},\eta)\cos[n(\varphi-\Psi_n)]\right\}, \quad (1)$$

where E, p, $p_{\rm T}$, φ and η are the particle's energy, momentum, transverse momentum, azimuthal angle and pseudorapidity, respectively, and Ψ_n is the azimuthal angle of the symmetry plane of the $n^{\rm th}$-order harmonic. v_n can be calculated as $v_n = \langle\cos[n(\varphi-\Psi_n)]\rangle$, where the brackets denote an average over all particles in all events. The anisotropic flow in heavy-ion collisions is understood as hydrodynamic response of produced matter to spatial deformations of the initial energy density profile [16]. This profile fluctuates event-by-event due to fluctuating position of the constituents inside the colliding nuclei, which implies that v_n also fluctuates [17, 18]. The recognition of the importance of flow fluctuations led to triangular and higher flow harmonics [19, 20] as well as to the correlation between different v_n harmonics [21, 22]. The higher order harmonics are expected to be sensitive to fluctuations in the initial conditions and to the magnitude of η/s [23, 24], while v_n correlations have the potential to discriminate between these two respective contributions [21].

Difficulties in extracting η/s in heavy-ion collisions can be attributed mostly to the fact that it strongly depends on the specific choice of the initial conditions [4, 24, 25]. The viscous effects reduce the magnitude of the elliptic flow. Furthermore, the magnitude of η/s used in hydrodynamic calculations should be considered as an average over the temperature evolution of the expanding fireball as it is known that η/s of other fluids depends on temperature. In addition, part of the elliptic flow can also originate from the hadronic phase [26–28]. Therefore, knowledge of both the temperature dependence of η/s and the relative contributions from the partonic and hadronic phases should be understood better to quantify η/s of the partonic fluid.

An important input to the hydrodynamic model simulations is the distribution of energy density in the

transverse plane (the initial density profile), which is usually estimated from the probability distribution of nucleons in the incoming nuclei. This initial energy density profile can be quantified by calculating the distribution of the spatial eccentricity [19],

$$\varepsilon_n e^{in\Phi_n} = -\{r^n e^{in\phi}\}/\{r^n\}, \quad (2)$$

where the curly brackets denote the average over the transverse plane, i.e., $\{\cdots\} = \int dxdy\ e(x,y,\tau_0)$ $(\cdots)$, r is the distance to the system's center of mass, $e(x,y,\tau_0)$ is the energy density at the initial time τ_0, and Φ_n is the participant plane angle (see Ref. [29, 30]). There are experimental and theoretical evidences [19, 20, 31] that the harmonic coefficients, v_2 and v_3, are to a good approximation linearly proportional to the deformations in the initial energy density in the transverse plane (e.g. $v_n \propto \varepsilon_n$ for n=2 or 3). v_4 and higher order flow coefficients can arise from initial anisotropies in the same harmonic [19, 29, 32, 33] (linear response) or can be induced by lower-order harmonics [34, 35] (nonlinear response). The higher harmonics ($n > 3$) could be understood as superpositions of linear and nonlinear responses, through which they are correlated with lower order harmonics [32, 33, 35, 36]. When the order of harmonic is large, the nonlinear response contribution in viscous hydrodynamics is dominant and become larger for more peripheral collisions [35, 36]. The magnitude of the viscous corrections as a function of p_T for v_4 and v_5 is sensitive to ansatz used for the viscous distribution function, a correction for the equilibrium distribution at hadronic freeze-out [36, 37]. Hence the studies of the higher order ($n > 3$) to lower order (v_2 or v_3) harmonic correlations and their p_T dependence can help to understand the viscous correction to the momentum distribution at hadronic freeze-out which is among the least understood parts of hydrodynamic calculations [30, 36].

Recently, ALICE Collaboration measured for the first time the new multiparticle observables, the Symmetric 2-harmonic 4-particle Cumulants (SC), which quantify the relationship between event-by-event fluctuations of two different flow harmonics [38]. The new observables are particularly robust against few-particle non-flow correlations and they provide independent information to recently analyzed symmetry plane correlators. It was demonstrated that they are sensitive to the temperature dependence of η/s of the expanding medium and therefore simultaneous descriptions of different order harmonic correlations would constrain both the initial conditions and the medium properties [38, 39]. In this article, we have extended the analysis of SC observables to higher order Fourier harmonics (up to 5$^{\text{th}}$ order) as well as to p_T dependence of correlations for the lower order harmonics (v_3-v_2 and v_4-v_2). We also include extensive comparisons to hydrodynamic and AMPT model calculations. In Sec. 2 we summarize our findings from the previous work [38] and present the analysis methods. The experimental setting and measurements are described in Sec. 3 and the sources of systematic uncertainties are explained in Sec. 4. The results of the measurements are presented in Sec. 5. In Sec. 6 we present comparisons to theoretical calculations. Various theoretical models used in the article are described in Sec. 6. Sec. 7 summarizes our findings.

2 Experimental Observables

The existing measurements provide an estimate of the average value of QGP's η/s both at RHIC and LHC energies. What remains uncertain is how the η/s of QGP depends on temperature (T). The temperature dependence of η/s in the QGP was discussed in [13]. The effects to hadron spectra and elliptic flow were studied in [40] for different parametrizations of $\eta/s(T)$. A more systematic study with the event-by-event EKRT+viscous hydrodynamic calculations has been just initiated in Ref. [30], where the first (and only rather qualitative) possibilities where investigated (see Fig. 1 therein). The emerging picture is that the study of individual flow harmonics v_n will unlikely reveal the details of $\eta/s(T)$ dependence. It was demonstrated already in [30] that different $\eta/s(T)$ parameterizations can lead to the same centrality dependence of individual flow harmonics. In Ref. [21] new flow observables were introduced which quantify the degree of correlation between two different harmonics v_m and v_n. These new observables

have potential to discriminate the contributions to anisotropic flow development from initial conditions and from the transport properties of the QGP [21]. Therefore their measurements would provide the experimental constrains of the theoretical predictions for individual stages of heavy-ion evolution independently. In addition, it turned out that correlations of different flow harmonics are sensitive to the temperature dependence of η/s [38], to which individual flow harmonics are weakly sensitive [30].

For reasons discussed in [38, 41], the correlations between different flow harmonics cannot be studied experimentally with the same set of observables introduced in [21]. Based on [41], the new flow observables obtained from multiparticle correlations, so-called *Symmetric Cumulants (SC)*, were introduced. SC observables are nearly insensitive to nonflow and quantify the correlation of amplitudes of two different flow harmonics. The first measurements of SC observables were recently published by ALICE Collaboration in [38].

The SC observables are defined as (for details see Sec. IV C in [41]):

$$\begin{aligned}\langle\langle\cos(m\varphi_1+n\varphi_2-m\varphi_3-n\varphi_4)\rangle\rangle_c &= \langle\langle\cos(m\varphi_1+n\varphi_2-m\varphi_3-n\varphi_4)\rangle\rangle \\ &\quad -\langle\langle\cos[m(\varphi_1-\varphi_2)]\rangle\rangle\langle\langle\cos[n(\varphi_1-\varphi_2)]\rangle\rangle \\ &= \langle v_m^2 v_n^2\rangle - \langle v_m^2\rangle\langle v_n^2\rangle\,, \end{aligned} \tag{3}$$

with the condition $m \neq n$ for two positive integers m and n. In this article SC(m,n) normalized with the product $\langle v_m^2\rangle\langle v_n^2\rangle$ [38, 42], is denoted by NSC(m,n):

$$\mathrm{NSC}(m,n) \equiv \frac{\mathrm{SC}(m,n)}{\langle v_m^2\rangle\langle v_n^2\rangle}\,. \tag{4}$$

Normalized symmetric cumulants reflect only the degree of the correlation which is expected to be insensitive to the magnitudes of v_m and v_n, while SC(m,n) contains both the degree of the correlations between two different flow harmonics and individual v_n harmonics. In Eq. (4) the products in the denominator are obtained with two-particle correlations using a pseudorapidity gap of $|\Delta\eta| > 1.0$ which suppresses biases from few-particle nonflow correlations. For the two two-particle correlations which appear in the definition of SC(m,n) in Eq. (3) the pseudorapidity gap is not needed, since nonflow is suppressed by construction in this case. This was verified by HIJING model simulations in [38].

The ALICE measurements [38] have revealed that fluctuations of v_2 and v_3 are anti-correlated, while fluctuations of v_2 and v_4 are correlated in all centralities [38]. However, the details of the centrality dependence differ in the fluctuation-dominated (most central) and the geometry-dominated (mid-central) regimes [38]. The observed centrality dependence of SC(4,2) cannot be captured with the constant η/s dependence, indicating clearly that the temperature dependence plays an important role. These results were also used to discriminate between different parameterizations of initial conditions. It was demonstrated that in the fluctuation-dominated regime (central collisions) MC-Glauber initial conditions with binary collisions weights are favored over wounded nucleon weights [38].

3 Data Analysis

A sample of Pb–Pb collisions at $\sqrt{s_{\mathrm{NN}}} = 2.76$ TeV recorded by ALICE during the 2010 heavy-ion run at the LHC is used for this analysis. Detailed descriptions of the ALICE detector can be found in [43–45]. The Time Projection Chamber (TPC) was used to reconstruct charged particle tracks and measure their momenta with full azimuthal coverage in the pseudorapidity range $|\eta| < 0.8$. Two scintillator arrays (V0) which cover the pseudo-rapidity ranges $-3.7 < \eta < -1.7$ and $2.8 < \eta < 5.1$ were used for triggering and the determination of centrality [46]. The trigger conditions and the event selection criteria are identical to those described in [2, 46]. Approximately 10^7 minimum-bias Pb–Pb events with a reconstructed primary vertex within ± 10 cm from the nominal interaction point in the beam direction are selected. Charged

particles reconstructed in the TPC in $|\eta| < 0.8$ and $0.2 < p_{\mathrm{T}} < 5$ GeV/c were selected. The charged track quality cuts described in [2] were applied to minimize contamination from secondary charged particles and fake tracks. The reconstruction efficiency and contamination ~~of charged particles~~ were estimated from HIJING Monte Carlo simulations [47] combined with a GEANT3 [48] detector model and were found to be independent of the collision centrality. The reconstruction efficiency increases from 70% to 80% for particles with $0.2 < p_{\mathrm{T}} < 1$ GeV/c and remains constant at $(80 \pm 5)\%$ for $p_{\mathrm{T}} > 1$ GeV/c. The estimated contamination by secondary charged particles from weak decays and photon conversions is less than 6% at $p_{\mathrm{T}} = 0.2$ GeV/c and falls below 1% for $p_{\mathrm{T}} > 1$ GeV/c. The p_{T} cut-off of 0.2 GeV/c reduces event-by-event biases due to small reconstruction efficiency at lower p_{T}, while the high p_{T} cut-off of 5 GeV/c reduces the ~~contribution to the anisotropies from jets.~~ Reconstructed TPC tracks were required to have at least 70 space points (out of a maximum of 159). Only tracks with a transverse distance of closest approach (DCA) to the primary vertex less than 3 mm, both in longitudinal and transverse directions, are accepted. This reduces the contamination from secondary tracks produced in the detector material, particles from weak decays, etc. Tracks with kinks (~~the~~ tracks that appear to change direction due to multiple scattering, $K^{\pm}$ decays) were rejected.

4 Systematic Uncertainties

The systematic uncertainties are estimated by varying the event and track selection criteria. All systematic checks described here are performed independently. ~~All results of SC(m,n) with a selected criterion~~ are compared to ones from the default event and track selection described in the previous section, ~~The differences between the default results and the ones obtained from the variation of the selection criteria~~ are taken as systematic uncertainty of each individual source. The contributions from different sources were added in quadrature to obtain the total systematic uncertainty.

The event centrality was determined by the V0 detectors [49] with better than 2% resolution. The systematic uncertainty from centrality determination was evaluated by using TPC and Silicon Pixel Detector (SPD) [50] detectors instead of V0 detectors. The systematic uncertainty from the centrality determinations is about 3% both for SC(5,2) and SC(4,3), and 8% for SC(5,3).

As described in Sec. 3, the reconstructed vertex position along the beam axis (z-vertex) is required to be located within 10 cm of interaction point (IP) to ensure a uniform detector acceptance for the tracks within $|\eta| < 0.8$ ~~for all the vertices~~. The systematic uncertainty from z-vertex cut was estimated by reducing the z-vertex to 8cm and was found to be less than 3%.

The analyzed events were recorded with two settings of the L3 magnet polarity and the resulting data sets have almost ~~the same~~ numbers of events. Events with both magnet polarity were used for the default analysis and the systematic uncertainties were evaluated from variation between each of two magnetic field settings. ~~Moreover, the effects from p_{T} dependence reconstruction efficiency were taken into systematic uncertainty.~~ Magnetic polarity variation and reconstruction efficiency effects are less than 2%.

The systematic uncertainty due to the track reconstruction was estimated from comparison between results for the so-called standalone TPC tracks with the same parameters as described in Sec. 3, and combination of the TPC and the Inner Tracking System (ITS) detectors with tighter selection criteria. To correct for non-uniform azimuthal acceptance due to dead zones in SPD, and to get the best transverse momentum resolution, approach of hybrid selection with SPD hit and/or ITS refit tracks combined with TPC were used. Then each track reconstruction was evaluated by varying the threshold on parameters used to select the tracks at the reconstruction level. The systematic difference of up to 12% was observed in SC(m,n) from the different track selections. In addition, we applied the like-sign technique to estimate non-flow contributions in SC(m,n). The difference between results obtained by selecting all charged particles and results obtained after either selecting only positively or only negatively charged particles was the largest contribution to the systematic uncertainty and it is about 7% for SC(4,3) and 20% for

SC(5,3).

Another large contribution to the systematic uncertainty originates from the non-uniform reconstruction efficiency in azimuthal angle. In order to estimate its effects, we use the AMPT model (see Sec. 6) which have flat uniform distribution of azimuthal angles. Detector inefficiencies was introduced to mimic non-uniform azimuthal distribution in the data. For the observables SC(5,2), SC(5,3) and SC(4,3), variation due to non-uniform acceptance is about 9%, 17% and 11%, respectively. Overall, the systematic uncertainties are larger for the SC(5,3) and SC(5,2) than for the lower harmonics of SC(m,n). This is because v_n are decreasing with n increasing and becomes more sensitive to azimuthal modulation due to detector imperfections.

5 Results

The centrality dependence of the higher order harmonic correlations (SC(4,3), SC(5,2) and SC(5,3)) are presented in Fig. 1 and compared to the lower order harmonic correlations (SC(4,2) and SC(3,2)) which are taken from [38]. The correlation between v_3 and v_4 is negative, and similarly for v_3 and v_2, while the other correlations are all positive, which reveals that v_2 and v_5, v_3 and v_5 are correlated as v_2 and v_4, while v_3 and v_4 are anti-correlated as v_3 and v_2.

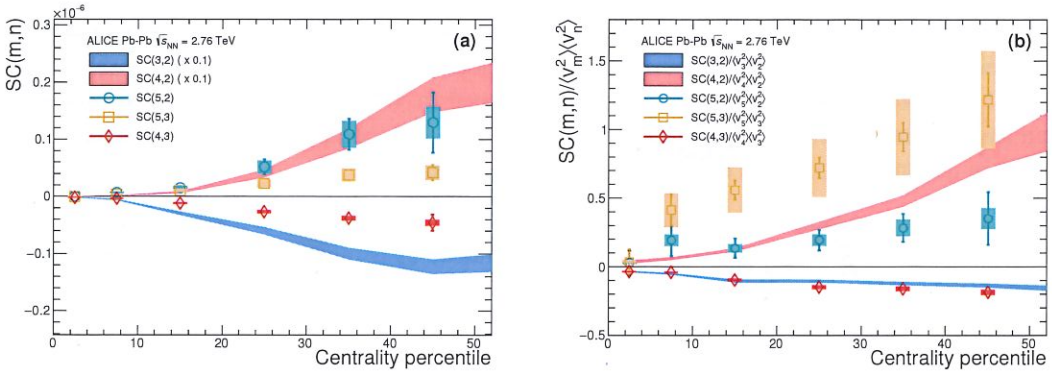

Fig. 1: SC(m,n) (a) and NSC(m,n) (b) with flow harmonic up to 5$^{\text{th}}$ order in Pb–Pb collisions at $\sqrt{s_{\text{NN}}} = 2.76$ TeV. The lower order harmonic correlations (SC(3,2), SC(4,2), NSC(3,2) and NSC(4,2)) are taken from [38] and shown as bands. Note that the systematic and statistical errors are combined quadratically for these lower order harmonic correlations and SC(4,2) and SC(3,2) on the panel (a) are scaled by factor of 0.1.

The higher order flow harmonic correlations (SC(4,3), SC(5,2) and SC(5,3)) are much smaller compared to the lower order harmonic correlations (SC(3,2) and SC(4,2)). In particular SC(5,2) is 10 times smaller than SC(4,2) and SC(4,3) is about 20 times smaller that SC(3,2).

However, unlike SC(m,n), the NSC(m,n) results with the higher order flow harmonics show almost the same order of the correlation strength as the lower order flow harmonic correlations (NSC(3,2) or NSC(4,2)). NSC(4,3) magnitude is comparable to NSC(3,2) and one finds that a hierarchy, NSC(5,3) > NSC(4,2) > NSC(5,2), holds for centrality ranges > 20% within the errors shown on the panel (b) in Fig. 1b. These results indicate that the lower order harmonic correlations (SC(3,2) and SC(4,2)) are larger than higher order harmonic correlations (SC(4,3), SC(5,2) and SC(5,3)), not only because of the correlation strength itself but also because of the strength of individual flow harmonics. SC(5,2) is stronger than SC(5,3), but as for NSC, the normalized correlation between v_5 and v_3 is stronger than the normalized correlation between v_5 and v_2.

It can be seen on the panel (a) in Fig. 1 that the lower order harmonic correlations (SC(3,2) and SC(4,2))